Acta Cryst E CRYSTALLOGRAPHIC COMMUNICATIONS

ISSN 2056-9890

The first coordination compound of 6-fluoronicotinate: the crystal structure of a one-dimensional nickel(II) coordination polymer containing the mixed ligands 6-fluoronicotinate and 4,4′-bipyridine

Received 4 February 2020
Accepted 3 March 2020

Edited by C. Massera, Università di Parma, Italy

Keywords: crystal structure; nickel(II); 6-fluoronicotinic acid; 4,4′-bipyridine; coordination polymer; hydrogen-bond motif.

CCDC reference: 1988000

Supporting information: this article has supporting information at journals.iucr.org/e

Nives Politeo,[a] Mateja Pisačić,[b] Marijana Đaković,[b] Vesna Sokol[a]* and Boris-Marko Kukovec[a]

[a]Department of Physical Chemistry, Faculty of Chemistry and Technology, University of Split, Ruđera Boškovića 35, HR-21000 Split, Croatia, and [b]Department of Chemistry, Faculty of Science, University of Zagreb, Horvatovac, 102a, HR-10000 Zagreb, Croatia. *Correspondence e-mail: vsokol@ktf-split.hr

A one-dimensional nickel(II) coordination polymer with the mixed ligands 6-fluoronicotinate (6-Fnic) and 4,4′-bipyridine (4,4′-bpy), namely, *catena*-poly[[diaquabis(6-fluoropyridine-3-carboxylato-κO)nickel(II)]-μ-4,4′-bipyridine-κ^2N:N'] trihydrate], $\{[Ni(6\text{-Fnic})_2(4,4'\text{-bpy})(H_2O)_2]\cdot 3H_2O\}_n$, (**1**), was prepared by the reaction of nickel(II) sulfate heptahydrate, 6-fluoronicotinic acid ($C_6H_4FNO_2$) and 4,4′-bipyridine ($C_{10}H_8N_2$) in a mixture of water and ethanol. The nickel(II) ion in **1** is octahedrally coordinated by the O atoms of two water molecules, two O atoms from *O*-monodentate 6-fluoronicotinate ligands and two N atoms from bridging 4,4′-bipyridine ligands, forming a *trans* isomer. The bridging 4,4′-bipyridine ligands connect symmetry-related nickel(II) ions into infinite one-dimensional polymeric chains running in the [1$\bar{1}$0] direction. In the extended structure of **1**, the polymeric chains and lattice water molecules are connected into a three-dimensional hydrogen-bonded network *via* strong O—H···O and O—H···N hydrogen bonds, leading to the formation of distinct hydrogen-bond ring motifs: octameric $R_8^8(24)$ and hexameric $R_8^6(16)$ loops.

1. Chemical context

The design of coordination polymers relies on the concepts of crystal engineering (Desiraju, 2007, 2013) and has become a prominent field of research in recent years for many reasons including the functional properties shown by coordination polymers, their aesthetics and many possible applications such as catalysis, gas storage and separation, magnetism, luminescence and molecular sensing (Mueller *et al.*, 2006; Bosch *et al.*, 2017; Zhang *et al.*, 2015; Zeng *et al.*, 2014, 2016; Douvali *et al.*, 2015; Xu *et al.*, 2017; Zhou *et al.*, 2017). The multifunctionality of the organic ligands used as building blocks in the assembly of coordination polymers is reflected in the position and coordination ability of their donor atoms and/or groups and is the main factor in the design of unusual and unexpected architectures with novel topologies and properties. The main challenge is to control the formation of a coordination polymer with the desired molecular and crystal structure, which is particularly affected by the experimental conditions such as the choice of solvents, starting metal salts, additional ligands, temperature, hydrothermal conditions, pH value (Li *et al.*, 2016; Zhou *et al.*, 2016; Gu *et al.*, 2016).

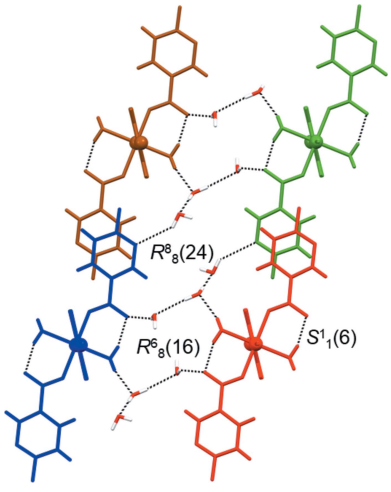

Various aromatic carboxylic acids with additional functional groups have often been used in the construction of coordination polymers because of the variety of their coordination modes (often unpredictable) and their potential for forming supramolecular interactions (Gu *et al.*, 2016, 2017, 2018; Wang *et al.*, 2016; Zhang *et al.*, 2019). Fluorine-substituted aromatic carboxylic acids are good candidates for the design of functional coordination polymers showing higher thermal stability as well as stability towards oxidation (Peikert *et al.*, 2015; Yuan *et al.*, 2016).

Although metal complexes with nicotinate have been well-studied and documented [almost 900 crystal structures in the Cambridge Structural Database (CSD, Version 5.40, searched January 2020; Groom *et al.*, 2016)], metal complexes of its fluorinated analogues (*e.g.* 5-fluoronicotinate) have been much less studied (around 30 crystal structures in the CSD). On the other hand, no metal complexes of other fluorinated analogues of nicotinate (*e.g.* 2-fluoronicotinate, 4-fluoronicotinate, 6-fluoronicotinate) have been reported so far.

Our goal was to prepare nickel(II) coordination polymers as the nickel(II) ion is relatively abundant, with a large ionic radius and defined stereochemistry, showing a high ligand-field stabilization energy, which enables the formation of nickel(II) coordination polymers with diverse topologies and high stabilities (Liu *et al.*, 2019). We opted for nickel(II) coordination polymers with mixed ligands: 6-fluoronicotinate (6-Fnic) as the main ligand and 4,4′-bipyridine (4,4′-bpy), a well-established, bridging N-donor ligand, frequently used in the design of nickel(II) coordination polymers, as the supporting ligand.

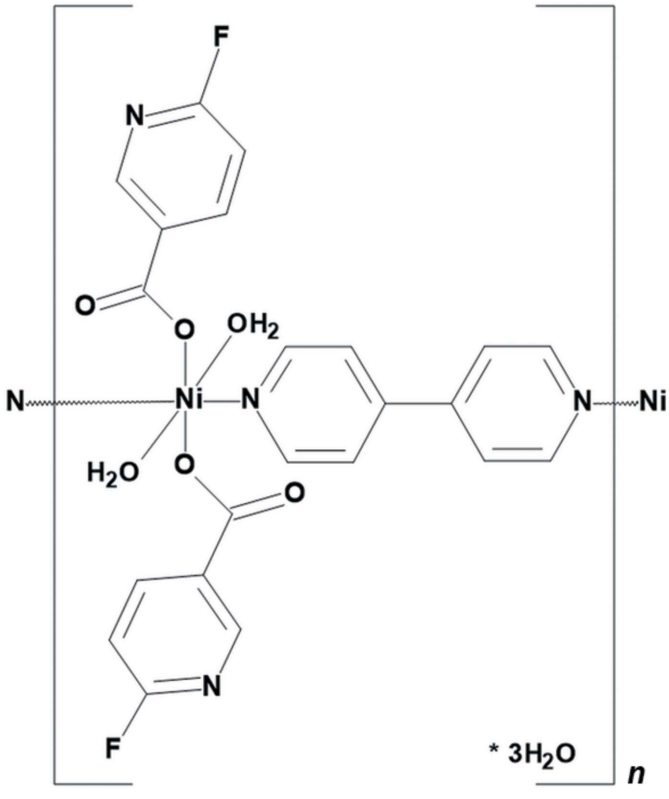

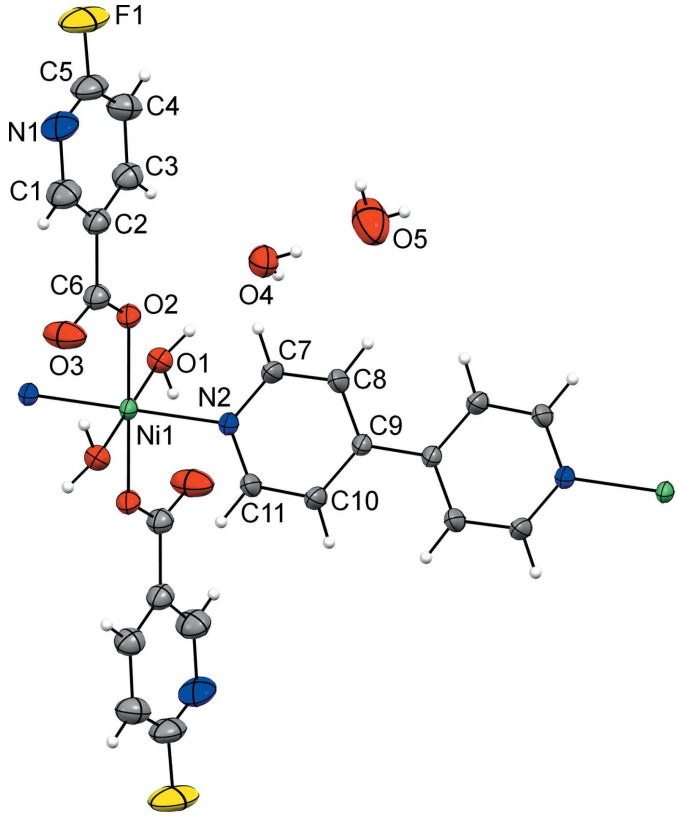

Figure 1
The repeating polymeric unit of **1**, showing the atomic numbering scheme of the asymmetric unit. The displacement ellipsoids are drawn at the 40% probability level.

In this work, we report the synthesis and characterization of the first metal complex with 6-fluoronicotinate – the one-dimensional nickel(II) coordination polymer {[Ni(6-Fnic)$_2$-(4,4′-bpy)(H$_2$O)$_2$]·3H$_2$O} (**1**). The synthesis was carried out in a mixture of water and ethanol in the hope that the coordinated water molecules would complete the coordination sphere around the nickel(II) ion and participate in the formation of various hydrogen-bond motifs within the hydrogen-bonded framework, along with the anticipated lattice water molecules. Furthermore, we wanted to explore the effect of the probable weak intermolecular interactions involving the aromatic F atoms (for example C—H···F interactions) on the assembly of the polymeric chains in the crystal packing.

2. Structural commentary

As the nickel(II) ion and the lattice water molecule (atom O4) are situated on an inversion center and a twofold axis, respectively, the asymmetric unit of **1** consists of one half of a nickel(II) ion, one coordinated water molecule, one fluoronicotinate ligand, one half of a 4,4′-bipyridine ligand and one and a half lattice water molecules. The nickel(II) ion is octahedrally coordinated by two 6-fluoronicotinate O atoms (O2 and O2^{i}) and by two 4,4′-bipyridine N atoms (N2 and N2^{i}) in the equatorial position, whilst two water molecule O atoms

Table 1
Hydrogen-bond geometry (Å, °).

D—H···A	D—H	H···A	D···A	D—H···A
O1—H12···O4	0.82 (1)	2.05 (1)	2.848 (2)	166 (2)
O1—H11···O3^{i}	0.82 (1)	1.88 (1)	2.674 (2)	163 (2)
O4—H41···O5^{ii}	0.82 (1)	1.99 (1)	2.811 (3)	175 (3)
O5—H51···O3^{iii}	0.82 (1)	2.24 (3)	2.964 (4)	147 (4)
O5—H52···N1^{iv}	0.82 (1)	2.41 (3)	3.100 (3)	142 (4)

Symmetry codes: (i) $-x+\frac{1}{2}, -y+\frac{3}{2}, -z$; (ii) $-x+1, y, -z+\frac{1}{2}$; (iii) $-x+\frac{1}{2}, y-\frac{1}{2}, -z+\frac{1}{2}$; (iv) $-x+\frac{1}{2}, -y+\frac{3}{2}, -z+1$.

(O1 and O1^{i}) are bound in the axial positions [symmetry code: (i) $-x+\frac{1}{2}, -y+\frac{3}{2}, -z$]. In this way, a *trans* isomer is formed (N2^{i}—Ni1—N2 = 180°) (Fig. 1). The 6-fluoronicotinate ligands are bound to the nickel(II) ion *via* their carboxylate O atoms in an *O*-monodentate fashion, whilst the 4,4′-bipyridine ligands act as bridge and, thus, connect the symmetry-related nickel(II) ions into an infinite one-dimensional polymeric chain extending in the [1$\bar{1}$0] direction (Fig. 2). There are three lattice water molecules per repeating polymeric unit, {[Ni(6-Fnic)$_2$(4,4′-bpy)(H$_2$O)$_2$]·3H$_2$O}.

The octahedral coordination environment around the nickel(II) ion is slightly distorted, as indicated by the angles for the *cis* pairs of the ligating atoms [89.65 (6)–90.87 (6)°]. The Ni1—O1 bond length [2.1067 (16) Å] is somewhat longer than the Ni1—O2 and Ni1—N2 bond lengths [2.0553 (13) and 2.0570 (16) Å, respectively], which is in agreement with the fact that the water molecules are bound in the axial positions of the octahedron. The Ni—O$_c$ (c = carboxylate) bond lengths in **1** are comparable to those seen in the related nickel(II) complexes with 6-chloronicotinate (Xia *et al.*, 2012), 5-fluoronicotinate (Cui *et al.*, 2015), mixed 5-fluoronicotinate and 2,2′-biimidazole ligands (Li *et al.*, 2019), mixed 5-bromonicotinate and 1,1′-(5-methyl-1,3-phenylene)bis(1*H*-imidazole) ligands (Lv *et al.*, 2016), 5-chloronicotinate (Chen *et al.*, 2019) and mixed 5-chloronicotinate and 2,2′-biimidazole ligands (Chen *et al.*, 2019). The Ni—N bond lengths are in agreement with those reported for nickel(II) complexes containing bridging 4,4′-bipyridine ligands (Groom *et al.*, 2016).

The 4,4′-bypyridine ring is not coplanar with the coordinated water molecule atom O1, but it is rotated slightly (approximately 4°) about the Ni1—N2 bond, as is evident from the torsion angles Ni1—N2—C7—C8 [176.35 (19)°] and Ni1—N2—C11—C10 [−176.03 (18)°]. The values of these torsion angles ought to be 180° in the case of coplanarity of the 4,4′-bipyridine ring and the O1 atom of the coordinated water molecule.

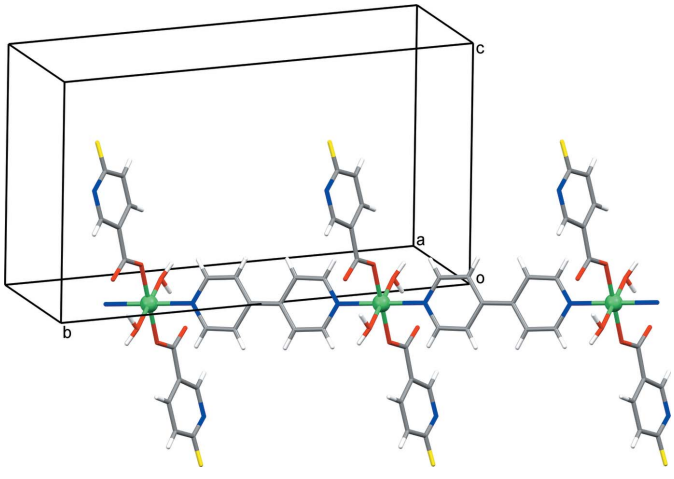

Figure 2
An infinite one-dimensional polymeric chain of **1** showing the connectivity.

3. Supramolecular features

The extended structure of **1** mainly features strong O—H···O and O—H···N hydrogen bonds (Table 1) and π–π interactions [*Cg*1···*Cg*1($-x+\frac{1}{2}, -y+\frac{3}{2}, -z+1$) = 3.8148 (16) Å; dihedral angle between the planes = 0.00 (14)°; slippage = 1.792 Å and *Cg*1···*Cg*2($x+\frac{1}{2}, 2-y, \frac{1}{2}+z$) = 3.8798 (16) Å; dihedral angle between the planes = 11.68 (13)°; slippage = 1.917 Å; *Cg*1 and *Cg*2 are the centroids of the 6-fluoronicotinate pyridine (N1/C1–C5) and 4,4′-bipyridine (N2/C7–C11) rings, respectively]. The strong hydrogen bonds link the polymeric chains and the lattice water molecules into an infinite three-dimensional network. The structure can be better analysed if viewed down the [1$\bar{1}$0] direction (the direction along which the polymeric chain is running). In that projection, the polymeric chains can be regarded as monomeric molecules that are interconnected with lattice water molecules into an infinite two-dimensional hydrogen-bonded network (Fig. 3). While being exclusively hydrogen-bonded to

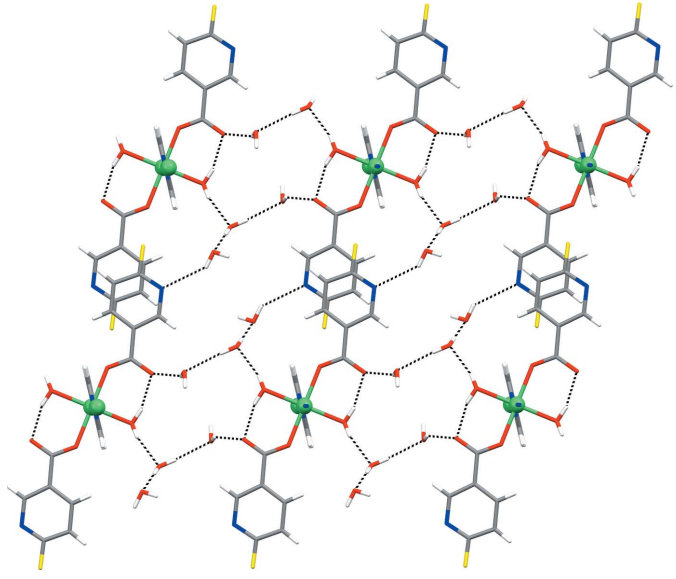

Figure 3
A fragment of the infinite two-dimensional hydrogen-bonded network of **1** viewed along the [1$\bar{1}$0] direction. The polymeric chains, represented as monomeric molecules in this projection, and lattice water molecules are connected by O—H···O and O—H···N hydrogen bonds (represented by dotted lines) within the network. The polymeric chains are additionally assembled by π–π interactions between symmetry-related 6-fluoronicotinate pyridine rings.

lattice water molecules, the polymeric chains are additionally directly assembled by π–π interactions between symmetry-related 6-fluoronicotinate pyridine rings [$Cg1\cdots Cg1$].

There are some distinctive hydrogen-bonded ring motifs within the two-dimensional network of **1** (Fig. 4). The octameric $R_8^8(24)$ motif is formed between six lattice water molecules and two symmetry-related polymeric chains (indicated in blue and green), which are linked *via* two 6-fluoronicotinate pyridine N atoms and two carboxylate O atoms. The hexameric $R_8^6(16)$ motif is formed between four lattice water molecules and two symmetry-related polymeric chains (indicated in blue and red), which are linked *via* two coordinated water molecules and two carboxylate O atoms, while the intramolecular $S_1^1(6)$ motif is formed within the polymeric chain (indicated in red) *via* a coordinated water molecule and a carboxylate O atom (Fig. 4). Both coordinated and lattice water molecules participate in the formation of motifs as single- and double-proton donors [coordinated water molecules as single-proton donors in the $S_1^1(6)$ motif and double-proton donors in the $R_8^6(16)$ motif; lattice water molecules as single-proton donors in the $R_8^8(24)$ and $R_8^6(16)$ motifs and double-proton donors in the $R_8^8(24)$ motif]. The 6-fluoronicotinate pyridine N atoms act as single-proton acceptors exclusively, while carboxylate O atoms act as both single- and double-proton acceptors [single in the $S_1^1(6)$ and $R_8^8(24)$ motifs and double in the $R_8^6(16)$ motif].

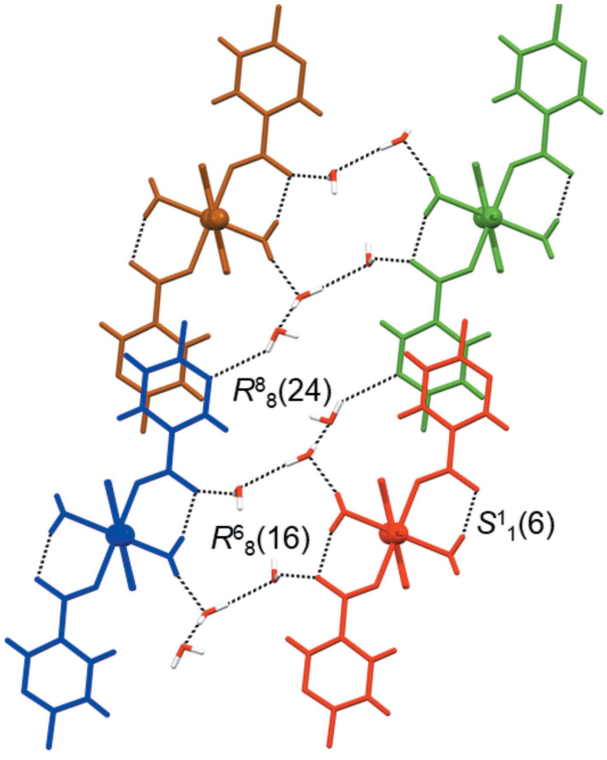

Figure 4
The distinctive hydrogen-bonded ring motifs (represented by the dotted lines) found within the two-dimensional network of **1** viewed along the [1$\bar{1}$0] direction, *viz*. octameric $R_8^8(24)$, hexameric $R_8^6(16)$ and intramolecular $S_1^1(6)$ motifs. The various symmetry-related polymeric chains (represented as momomeric molecules in this projection) are shown in brown, green, blue and red (see text).

Although there are many reported nickel(II) coordination polymers containing bridging 4,4′-bipyridine and pyridinedicarboxylate ligands, there are only two structurally similar one-dimensional nickel(II) polymers with 4,4′-bipyridine and pyridinecarboxylate (*i.e.* picolinate; Li *et al.*, 2009) or fluorinated benzoate (2,6-difluorobenzoate; Yuan *et al.*, 2016) ligands. The polymeric chains are assembled with lattice water molecules in the crystal packing of the picolinate polymer (Li *et al.*, 2009) or with the solvated ethanol molecules in the crystal packing of the 2,6-difluorobenzoate polymer (Yuan *et al.*, 2016). The discussed hydrogen-bond motifs in **1** are completely different from those observed in the crystal packings of these similar polymers, except for the intramolecular $S_1^1(6)$ motif, which is also present in the packing of the 2,6-difluorobenzoate polymer (Yuan *et al.*, 2016). The reason for the different hydrogen-bond motifs may be due to the different arrangement of the lattice water molecules (primarily connected to each other into a layered network and not extensively connected to the polymeric chains) in the packing of the picolinate polymer (Li *et al.*, 2009), and the fact that the ethanol O atoms are solely proton acceptors (not being able to participate in extensive hydrogen bonding as water molecules) in the packing of the 2,6-difluorobenzoate polymer (Yuan *et al.*, 2016).

Unfortunately, there are no weak intermolecular interactions involving the aromatic F atoms; we hoped these interactions could have an effect on the supramolecular assembly of the polymeric chains in **1**. The reason for the lack of such interactions may be the extensive hydrogen bonding, comprising strong O—H···O and O—H···N hydrogen bonds, that hinders weak C—H···F supramolecular interactions. Indeed, the crystallization from an aqueous solution enabled the participation of the lattice water molecules in the extended structure of **1**, enhancing the number of O—H···O and O—H···N hydrogen bonds in the hydrogen-bonded network and leading to the formation of the anticipated hydrogen-bond motifs.

4. PXRD and thermal analysis

The PXRD analysis was used to confirm the bulk content of **1** (Fig. 5). The experimental and calculated PXRD spectra of **1** are in very good agreement.

The thermal stability of **1**, as determined from the TG curve, is only up to 40°C (Fig. S1 in the supporting information). Both the coordinated (two) and lattice (three) water molecules were released in the same step (observed mass loss 14.5%, calculated 15.4%). The two small endothermic peaks in the DSC curve (63 and 115°C) suggest that the process of the water evolution is not straightforward and that the water molecules are differently bound in **1** (coordinated *vs* lattice). Indeed, the polymeric chains and lattice water molecules are assembled into a hydrogen-bonded three-dimensional structure (see *Supramolecular features*). It is therefore not surprising that the release of some water molecules affects the whole hydrogen-bonded structure and leads to its complete collapse in a single, not well-resolved thermal step. The

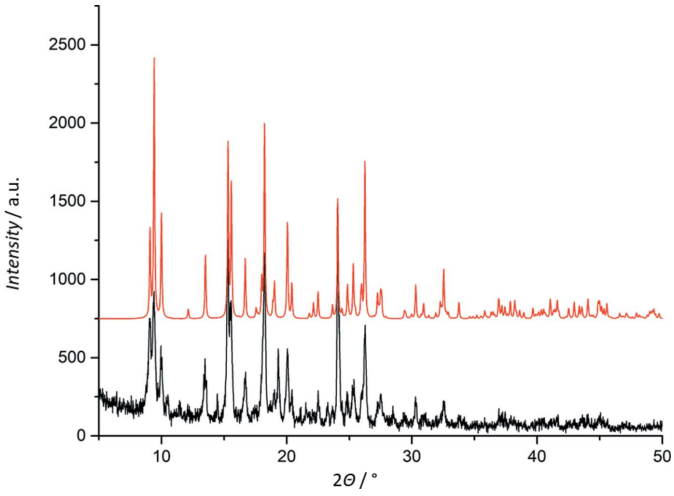

Figure 5
Experimental (bottom) and calculated (top) PXRD spectra of **1**.

thermal decomposition of **1** continues in a broad step (observed mass loss 56.7%) in the wide temperature range of 150–570°C (without any well-defined peaks in the DSC curve), which probably corresponds to the complete degradation of **1**. The remaining residue at 600°C is most probably NiO.

5. Materials and methods

All chemicals for the synthesis were purchased from commercial sources (Merck, ChemPUR) and used as received without further purification. The IR spectrum was obtained in the range 4000–400 cm^{-1} on a Perkin–Elmer Spectrum Two™ FTIR spectrometer in the ATR mode. The PXRD trace was recorded on a Philips PW 1850 diffractometer, Cu $K\alpha$ radiation, voltage 40 kV, current 40 mA, in the angle range 5–50° (2θ) with a step size of 0.02°. Simultaneous TGA/DSC measurements were performed at a heating rate of 10°C min^{-1} in the temperature range 25–600°C, under a nitrogen flow of 50 mL min^{-1} on an Mettler-Toledo TGA/DSC 3+ instrument. Approximately 2 mg of the sample were placed in a standard alumina crucible (70 µl).

6. Synthesis and crystallization

6-Fluoronicotinic acid (0.0495 g, 0.3508 mmol) was dissolved in distilled water (5 ml), 4,4′-bipyridine (0.0276 g, 0.1767 mmol) was dissolved in ethanol (2 mL) and nickel(II) sulfate heptahydrate (0.0517 g, 0.1841 mmol) was dissolved in distilled water (2 mL). The solutions of the two ligands were first mixed together under stirring. The resulting solution was then slowly added to the nickel(II) sulfate solution under stirring. The pH of the final solution was adjusted to 7 by adding an ammonia solution dropwise. The obtained, clear solution was left to evaporate slowly at room temperature for approximately three weeks until light–blue crystals of **1**, suitable for X-ray diffraction measurements, were obtained. These were collected by filtration, washed with their mother liquor and dried *in vacuo*. Yield: 0.0483 g (45%). Selected IR bands (ATR) (ν, cm^{-1}): 3351 [ν(O—H)], 3088 [ν(C—H)], 1607 [ν(C═O)], 1558, 1475, 1415, 1392, 1368 [ν(C—C), ν(C—N)] (see Fig. S2, Table S1 in the supporting information).

Table 2
Experimental details.

Crystal data	
Chemical formula	$\{[Ni(C_6H_3FNO_2)_2(C_{10}H_8N_2)(H_2O)_2]\cdot 3H_2O\}_n$
M_r	585.16
Crystal system, space group	Monoclinic, *C*2/*c*
Temperature (K)	296
a, *b*, *c* (Å)	12.1175 (5), 18.7705 (6), 12.3246 (4)
β (°)	110.232 (4)
V (Å^3)	2630.29 (17)
Z	4
Radiation type	Mo $K\alpha$
μ (mm^{-1})	0.81
Crystal size (mm)	0.15 × 0.10 × 0.08
Data collection	
Diffractometer	Oxford Diffraction Xcalibur2 diffractometer with Sapphire 3 CCD detector
Absorption correction	Multi-scan (*CrysAlis PRO*; Rigaku, 2018)
T_{min}, T_{max}	0.899, 1.000
No. of measured, independent and observed [$I > 2\sigma(I)$] reflections	5540, 2316, 1960
R_{int}	0.032
$(\sin\theta/\lambda)_{max}$ (Å^{-1})	0.595
Refinement	
$R[F^2 > 2\sigma(F^2)]$, $wR(F^2)$, S	0.032, 0.073, 1.03
No. of reflections	2316
No. of parameters	189
No. of restraints	7
H-atom treatment	H atoms treated by a mixture of independent and constrained refinement
$\Delta\rho_{max}$, $\Delta\rho_{min}$ (e Å^{-3})	0.30, −0.22

Computer programs: *CrysAlis PRO* (Rigaku, 2018), *SHELXT* (Sheldrick, 2015*a*), *SHELXL2018/3* (Sheldrick, 2015*b*) and *Mercury* (Macrae *et al.*, 2020).

7. Refinement

Crystal data, data collection and structure refinement details are summarized in Table 2. C-bound atoms were positioned geometrically and refined using a riding model [0.93 Å, U_{iso}(H) = 1.2U_{eq}(C) for aromatic H atoms]. Water H atoms were found in difference-Fourier maps, O—H distances were restrained to an average value of 0.82 Å using DFIX and DANG instructions and they were refined isotropically [U_{iso}(H) = 1.2U_{eq}(O)].

The highest difference peak is 0.92 Å away from the O3 atom and the deepest difference hole is 0.50 Å away from the Ni1 atom.

Funding information

This research was supported by a grant from the Foundation of the Croatian Academy of Sciences and Arts for 2019 and by the University of Split institutional funding.

References

Bosch, M., Yuan, S., Rutledge, W. & Zhou, H.-C. (2017). *Acc. Chem. Res.* **50**, 857–865.

Chen, J.-W., Li, Y., Zou, X.-Z., Qiu, W.-D. & Cheng, X.-L. (2019). *Chin. J. Inorg. Chem.* **35**, 505–514.

Cui, Y.-H., Wu, J., Kirillov, A. M., Gu, J.-Z. & Dou, W. (2015). *RSC Adv.* **5**, 10400–10411.

Desiraju, G. R. (2007). *Angew. Chem. Int. Ed.* **46**, 8342–8356.

Desiraju, G. R. (2013). *J. Am. Chem. Soc.* **135**, 9952–9967.

Douvali, A., Tsipis, A. C., Eliseeva, S. V., Petoud, S., Papaefstathiou, G. S., Malliakas, C. D., Papadas, I., Armatas, G. S., Margiolaki, I., Kanatzidis, M. G., Lazarides, T. & Manos, M. J. (2015). *Angew. Chem. Int. Ed.* **54**, 1651–1656.

Groom, C. R., Bruno, I. J., Lightfoot, M. P. & Ward, S. C. (2016). *Acta Cryst.* B**72**, 171–179.

Gu, J., Cui, Y., Liang, X., Wu, J., Lv, D. & Kirillov, A. M. (2016). *Cryst. Growth Des.* **16**, 4658–4670.

Gu, J.-Z., Cai, Y., Liang, X.-X., Wu, J., Shi, Z.-F. & Kirillov, A. M. (2018). *CrystEngComm*, **20**, 906–916.

Gu, J.-Z., Liang, X.-X., Cai, Y., Wu, J., Shi, Z.-F. & Kirillov, A. M. (2017). *Dalton Trans.* **46**, 10908–10925.

Li, J.-J., Fan, T.-T., Qu, X.-L., Han, H.-L. & Li, X. (2016). *Dalton Trans.* **45**, 2924–2935.

Li, X.-M., Niu, Y.-L., Wang, Q.-W., Liu, B., Zhao, X. & Li, D. (2009). *Chin. J. Struct. Chem.* **28**, 321–324.

Li, Y., Zou, X.-Z., Qiu, W.-D., Feng, A.-S. & Chen, X.-L. (2019). *Chin. J. Struct. Chem.* **38**, 999–1011.

Liu, H., Kang, Y.-F., Fan, Y.-P., Guo, F.-S., Liu, L., Li, J.-L., Liu, P. & Wang, Y.-Y. (2019). *Cryst. Growth Des.* **19**, 797–807.

Lv, L.-L., Zhang, L.-J., Zhao, H. & Wu, B.-L. (2016). *Polyhedron*, **115**, 204–211.

Macrae, C. F., Sovago, I., Cottrell, S. J., Galek, P. T. A., McCabe, P., Pidcock, E., Platings, M., Shields, G. P., Stevens, J. S., Towler, M. & Wood, P. A. (2020). *J. Appl. Cryst.* **53**, 226–235.

Mueller, U., Schubert, M., Teich, F., Puetter, H., Schierle-Arndt, K. & Pastré, J. (2006). *J. Mater. Chem.* **16**, 626–636.

Peikert, K., Hoffmann, F. & Fröba, M. (2015). *CrystEngComm*, **17**, 353–360.

Rigaku (2018). *CrysAlis PRO*. Rigaku Inc., Tokyo, Japan.

Sheldrick, G. M. (2015*a*). *Acta Cryst.* A**71**, 3–8.

Sheldrick, G. M. (2015*b*). *Acta Cryst.* C**71**, 3–8.

Wang, H.-H., Yang, H.-Y., Shu, C.-H., Chen, Z.-Y., Hou, L. & Wang, Y.-Y. (2016). *Cryst. Growth Des.* **16**, 5394–5402.

Xia, Q.-H., Guo, Z.-F., Liu, L., Lv, J.-Q. & Li, B. (2012). *Acta Cryst.* E**68**, m1393.

Xu, M., Yuan, S., Chen, X.-Y., Chang, Y.-J., Day, G., Gu, Z.-Y. & Zhou, H.-C. (2017). *J. Am. Chem. Soc.* **139**, 8312–8319.

Yuan, H.-Q., Xiao, W., Hu, C.-Y. & Bao, G.-M. (2016). *Z. Kristallogr. New Cryst. Struct.* **231**, 125–127.

Zeng, M.-H., Yin, Z., Liu, Z.-H., Xu, H.-B., Feng, Y.-C., Hu, Y.-Q., Chang, L.-X., Zhang, Y.-X., Huang, J. & Kurmoo, M. (2016). *Angew. Chem. Int. Ed.* **55**, 11407–11411.

Zeng, M.-H., Yin, Z., Tan, Y.-X., Zhang, W.-X., He, Y.-P. & Kurmoo, M. (2014). *J. Am. Chem. Soc.* **136**, 4680–4688.

Zhang, W.-X., Liao, P.-Q., Lin, R.-B., Wei, Y.-S., Zeng, M.-H. & Chen, X.-M. (2015). *Coord. Chem. Rev.* **293–294**, 263–278.

Zhang, Y.-X., Lin, H., Wen, Y. & Zhu, Q.-L. (2019). *Cryst. Growth Des.* **19**, 1057–1063.

Zhou, H.-F., He, T., Yue, K.-F., Liu, Y.-L., Zhou, C.-S., Yan, N. & Wang, Y.-Y. (2016). *Cryst. Growth Des.* **16**, 3961–3968.

Zhou, Z., He, C., Yang, L., Wang, Y., Liu, T. & Duan, C. (2017). *ACS Catal.* **7**, 2248–2256.

supporting information

Acta Cryst. (2020). E**76**, 500-505 [https://doi.org/10.1107/S2056989020003023]

The first coordination compound of 6-fluoronicotinate: the crystal structure of a one-dimensional nickel(II) coordination polymer containing the mixed ligands 6-fluoronicotinate and 4,4′-bipyridine

Nives Politeo, Mateja Pisačić, Marijana Đaković, Vesna Sokol and Boris-Marko Kukovec

Computing details

Data collection: *CrysAlis PRO* (Rigaku, 2018); cell refinement: *CrysAlis PRO* (Rigaku, 2018); data reduction: *CrysAlis PRO* (Rigaku, 2018); program(s) used to solve structure: SHELXT (Sheldrick, 2015*a*); program(s) used to refine structure: *SHELXL2018/3* (Sheldrick, 2015*b*); molecular graphics: *Mercury* (Macrae *et al.*, 2020); software used to prepare material for publication: *SHELXL2018/3* (Sheldrick, 2015*b*).

***catena*-Poly[[diaquabis(6-fluoropyridine-3-carboxylato-κO)nickel(II)]-μ-4,4′-bipyridine-κ^2N:N'] trihydrate]**

Crystal data

$[Ni(C_6H_3FNO_2)_2(C_{10}H_8N_2)(H_2O)_2]\cdot 3H_2O$
$M_r = 585.16$
Monoclinic, $C2/c$
$a = 12.1175$ (5) Å
$b = 18.7705$ (6) Å
$c = 12.3246$ (4) Å
$\beta = 110.232$ (4)°
$V = 2630.29$ (17) Å^3
$Z = 4$
$F(000) = 1208$
$D_x = 1.478$ Mg m^{-3}
Mo $K\alpha$ radiation, $\lambda = 0.71073$ Å
Cell parameters from 2838 reflections
$\theta = 4.6$–$31.4°$
$\mu = 0.81$ mm^{-1}
$T = 296$ K
Prism, light-blue
0.15 × 0.10 × 0.08 mm

Data collection

Oxford Diffraction Xcalibur2 diffractometer with Sapphire 3 CCD detector
ω–scan
Absorption correction: multi-scan (CrysAlisPro; Rigaku, 2018)
$T_{min} = 0.899$, $T_{max} = 1.000$
5540 measured reflections
2316 independent reflections
1960 reflections with $I > 2\sigma(I)$
$R_{int} = 0.032$
$\theta_{max} = 25.0°$, $\theta_{min} = 4.1°$
$h = -13\rightarrow14$
$k = -22\rightarrow16$
$l = -14\rightarrow12$

Refinement

Refinement on F^2
Least-squares matrix: full
$R[F^2 > 2\sigma(F^2)] = 0.032$
$wR(F^2) = 0.073$
$S = 1.02$
2316 reflections
189 parameters
7 restraints
Hydrogen site location: mixed
H atoms treated by a mixture of independent and constrained refinement
$w = 1/[\sigma^2(F_o^2) + (0.033P)^2 + 1.7768P]$ where $P = (F_o^2 + 2F_c^2)/3$
$(\Delta/\sigma)_{max} < 0.001$
$\Delta\rho_{max} = 0.30$ e Å^{-3}
$\Delta\rho_{min} = -0.22$ e Å^{-3}

Special details

Geometry. All esds (except the esd in the dihedral angle between two l.s. planes) are estimated using the full covariance matrix. The cell esds are taken into account individually in the estimation of esds in distances, angles and torsion angles; correlations between esds in cell parameters are only used when they are defined by crystal symmetry. An approximate (isotropic) treatment of cell esds is used for estimating esds involving l.s. planes.

Fractional atomic coordinates and isotropic or equivalent isotropic displacement parameters (Å²)

	x	*y*	*z*	U_{iso}*/U_{eq}
Ni1	0.250000	0.750000	0.000000	0.02551 (12)
N1	0.2304 (2)	0.89116 (14)	0.49414 (19)	0.0627 (7)
N2	0.16406 (15)	0.65554 (9)	0.00035 (13)	0.0283 (4)
O1	0.41435 (14)	0.69897 (8)	0.06960 (13)	0.0365 (4)
H12	0.429 (2)	0.6719 (11)	0.1244 (14)	0.044*
H11	0.416 (2)	0.6772 (11)	0.0127 (14)	0.044*
O2	0.25264 (13)	0.77061 (8)	0.16466 (12)	0.0349 (4)
O3	0.12044 (17)	0.85740 (11)	0.13890 (14)	0.0661 (6)
O4	0.500000	0.59666 (15)	0.250000	0.0563 (7)
H41	0.539 (2)	0.5710 (13)	0.223 (3)	0.068*
O5	0.3692 (3)	0.51516 (15)	0.3540 (2)	0.1055 (9)
H51	0.401 (4)	0.4760 (12)	0.372 (3)	0.127*
H52	0.374 (4)	0.533 (2)	0.416 (2)	0.127*
F1	0.35722 (18)	0.86788 (12)	0.67067 (13)	0.0934 (6)
C1	0.1919 (3)	0.87822 (15)	0.3797 (2)	0.0542 (7)
H1	0.128197	0.904258	0.332209	0.065*
C2	0.2426 (2)	0.82806 (12)	0.32961 (19)	0.0385 (5)
C3	0.3359 (2)	0.78930 (14)	0.4018 (2)	0.0438 (6)
H3	0.371596	0.754740	0.371012	0.053*
C4	0.3763 (2)	0.80150 (16)	0.5186 (2)	0.0527 (7)
H4	0.438816	0.776057	0.569207	0.063*
C5	0.3193 (3)	0.85305 (17)	0.5559 (2)	0.0600 (8)
C6	0.2003 (2)	0.81802 (12)	0.20071 (19)	0.0373 (5)
C7	0.1834 (2)	0.61732 (12)	0.09598 (18)	0.0420 (6)
H7	0.240902	0.632605	0.163889	0.050*
C8	0.1220 (2)	0.55619 (12)	0.09870 (19)	0.0452 (6)
H8	0.138908	0.530975	0.167511	0.054*
C9	0.03574 (17)	0.53205 (10)	0.00029 (16)	0.0266 (4)
C10	0.0173 (2)	0.57183 (12)	−0.09902 (18)	0.0377 (5)
H10	−0.039219	0.557751	−0.168379	0.045*
C11	0.0828 (2)	0.63211 (12)	−0.09476 (17)	0.0375 (5)
H11A	0.069114	0.657839	−0.162659	0.045*

Atomic displacement parameters (Å²)

	U^{11}	U^{22}	U^{33}	U^{12}	U^{13}	U^{23}
Ni1	0.0328 (2)	0.0207 (2)	0.02366 (19)	−0.00983 (16)	0.01060 (15)	−0.00195 (14)
N1	0.0853 (19)	0.0660 (16)	0.0442 (13)	−0.0026 (14)	0.0320 (14)	−0.0202 (11)
N2	0.0347 (9)	0.0245 (9)	0.0257 (9)	−0.0092 (7)	0.0103 (8)	−0.0014 (7)

O1	0.0415 (9)	0.0348 (9)	0.0312 (8)	−0.0032 (7)	0.0101 (7)	0.0016 (6)
O2	0.0493 (9)	0.0301 (8)	0.0292 (8)	−0.0061 (7)	0.0183 (7)	−0.0036 (6)
O3	0.0746 (13)	0.0801 (14)	0.0386 (10)	0.0310 (12)	0.0133 (10)	−0.0040 (9)
O4	0.0750 (19)	0.0426 (16)	0.0524 (16)	0.000	0.0233 (14)	0.000
O5	0.173 (3)	0.0724 (18)	0.101 (2)	0.0023 (18)	0.085 (2)	0.0076 (15)
F1	0.1125 (15)	0.1310 (18)	0.0359 (9)	−0.0144 (13)	0.0247 (10)	−0.0284 (10)
C1	0.0651 (17)	0.0574 (17)	0.0441 (14)	0.0054 (14)	0.0239 (13)	−0.0079 (12)
C2	0.0444 (13)	0.0405 (14)	0.0350 (12)	−0.0078 (11)	0.0194 (11)	−0.0058 (10)
C3	0.0456 (13)	0.0506 (16)	0.0393 (13)	−0.0050 (12)	0.0200 (11)	−0.0038 (11)
C4	0.0487 (15)	0.072 (2)	0.0356 (13)	−0.0083 (13)	0.0128 (12)	0.0001 (12)
C5	0.073 (2)	0.078 (2)	0.0317 (14)	−0.0204 (17)	0.0214 (14)	−0.0136 (13)
C6	0.0427 (13)	0.0384 (13)	0.0325 (12)	−0.0056 (11)	0.0153 (11)	−0.0033 (10)
C7	0.0527 (14)	0.0393 (14)	0.0252 (11)	−0.0246 (11)	0.0022 (10)	0.0008 (9)
C8	0.0619 (15)	0.0379 (14)	0.0273 (11)	−0.0245 (12)	0.0047 (11)	0.0071 (10)
C9	0.0331 (10)	0.0226 (11)	0.0243 (10)	−0.0065 (8)	0.0103 (9)	−0.0025 (8)
C10	0.0444 (13)	0.0368 (13)	0.0267 (11)	−0.0196 (10)	0.0057 (10)	−0.0013 (9)
C11	0.0478 (13)	0.0351 (13)	0.0256 (11)	−0.0181 (11)	0.0074 (10)	0.0051 (9)

Geometric parameters (Å, º)

Ni1—O2^{i}	2.0553 (13)	F1—C5	1.357 (3)
Ni1—O2	2.0553 (13)	C1—C2	1.381 (3)
Ni1—N2^{i}	2.0570 (16)	C1—H1	0.9300
Ni1—N2	2.0570 (16)	C2—C3	1.380 (3)
Ni1—O1^{i}	2.1067 (16)	C2—C6	1.503 (3)
Ni1—O1	2.1067 (16)	C3—C4	1.370 (3)
N1—C5	1.298 (4)	C3—H3	0.9300
N1—C1	1.345 (3)	C4—C5	1.358 (4)
N2—C11	1.319 (3)	C4—H4	0.9300
N2—C7	1.330 (3)	C7—C8	1.374 (3)
O1—H12	0.815 (10)	C7—H7	0.9300
O1—H11	0.819 (9)	C8—C9	1.376 (3)
O2—C6	1.260 (3)	C8—H8	0.9300
O3—C6	1.246 (3)	C9—C10	1.384 (3)
O4—H41	0.822 (10)	C9—C9^{iii}	1.481 (4)
O4—H41^{ii}	0.822 (10)	C10—C11	1.373 (3)
O5—H51	0.823 (10)	C10—H10	0.9300
O5—H52	0.820 (10)	C11—H11A	0.9300
O2^{i}—Ni1—O2	180.00 (8)	C3—C2—C6	121.3 (2)
O2^{i}—Ni1—N2^{i}	89.73 (6)	C1—C2—C6	121.1 (2)
O2—Ni1—N2^{i}	90.27 (6)	C4—C3—C2	120.3 (2)
O2^{i}—Ni1—N2	90.27 (6)	C4—C3—H3	119.9
O2—Ni1—N2	89.73 (6)	C2—C3—H3	119.9
N2^{i}—Ni1—N2	180.0	C5—C4—C3	115.9 (3)
O2^{i}—Ni1—O1^{i}	89.65 (6)	C5—C4—H4	122.1
O2—Ni1—O1^{i}	90.35 (6)	C3—C4—H4	122.1
N2^{i}—Ni1—O1^{i}	90.87 (6)	N1—C5—F1	114.3 (3)

N2—Ni1—O1^{i}	89.13 (6)	N1—C5—C4	127.6 (2)
O2^{i}—Ni1—O1	90.35 (6)	F1—C5—C4	118.1 (3)
O2—Ni1—O1	89.65 (6)	O3—C6—O2	125.6 (2)
N2^{i}—Ni1—O1	89.13 (6)	O3—C6—C2	118.7 (2)
N2—Ni1—O1	90.87 (6)	O2—C6—C2	115.6 (2)
O1^{i}—Ni1—O1	180.0	N2—C7—C8	122.8 (2)
C5—N1—C1	115.6 (2)	N2—C7—H7	118.6
C11—N2—C7	117.17 (18)	C8—C7—H7	118.6
C11—N2—Ni1	120.57 (13)	C7—C8—C9	120.4 (2)
C7—N2—Ni1	122.19 (14)	C7—C8—H8	119.8
Ni1—O1—H12	122.0 (17)	C9—C8—H8	119.8
Ni1—O1—H11	100.5 (17)	C8—C9—C10	116.28 (18)
H12—O1—H11	110 (2)	C8—C9—C9^{iii}	122.5 (2)
C6—O2—Ni1	130.05 (14)	C10—C9—C9^{iii}	121.2 (2)
H41—O4—H41^{ii}	108 (4)	C11—C10—C9	119.77 (19)
H51—O5—H52	103 (3)	C11—C10—H10	120.1
N1—C1—C2	123.0 (3)	C9—C10—H10	120.1
N1—C1—H1	118.5	N2—C11—C10	123.57 (19)
C2—C1—H1	118.5	N2—C11—H11A	118.2
C3—C2—C1	117.6 (2)	C10—C11—H11A	118.2

C5—N1—C1—C2	−0.2 (4)	C1—C2—C6—O3	2.1 (3)
N1—C1—C2—C3	0.9 (4)	C3—C2—C6—O2	2.5 (3)
N1—C1—C2—C6	−177.0 (2)	C1—C2—C6—O2	−179.8 (2)
C1—C2—C3—C4	−0.7 (4)	C11—N2—C7—C8	−0.6 (4)
C6—C2—C3—C4	177.2 (2)	Ni1—N2—C7—C8	176.35 (19)
C2—C3—C4—C5	−0.2 (4)	N2—C7—C8—C9	−0.4 (4)
C1—N1—C5—F1	179.2 (2)	C7—C8—C9—C10	1.1 (3)
C1—N1—C5—C4	−0.9 (4)	C7—C8—C9—C9^{iii}	−177.8 (3)
C3—C4—C5—N1	1.1 (4)	C8—C9—C10—C11	−0.8 (3)
C3—C4—C5—F1	−179.0 (2)	C9^{iii}—C9—C10—C11	178.1 (2)
Ni1—O2—C6—O3	11.0 (3)	C7—N2—C11—C10	1.0 (3)
Ni1—O2—C6—C2	−166.92 (13)	Ni1—N2—C11—C10	−176.03 (18)
C3—C2—C6—O3	−175.6 (2)	C9—C10—C11—N2	−0.3 (4)

Symmetry codes: (i) −*x*+1/2, −*y*+3/2, −*z*; (ii) −*x*+1, *y*, −*z*+1/2; (iii) −*x*, −*y*+1, −*z*.

Hydrogen-bond geometry (Å, º)

D—H···*A*	*D*—H	H···*A*	*D*···*A*	*D*—H···*A*
O1—H12···O4	0.82 (1)	2.05 (1)	2.848 (2)	166 (2)
O1—H11···O3^{i}	0.82 (1)	1.88 (1)	2.674 (2)	163 (2)
O4—H41···O5^{ii}	0.82 (1)	1.99 (1)	2.811 (3)	175 (3)
O5—H51···O3^{iv}	0.82 (1)	2.24 (3)	2.964 (4)	147 (4)
O5—H52···N1^{v}	0.82 (1)	2.41 (3)	3.100 (3)	142 (4)
C11—H11*A*···O2^{i}	0.93	2.55	3.040 (2)	113

Symmetry codes: (i) −*x*+1/2, −*y*+3/2, −*z*; (ii) −*x*+1, *y*, −*z*+1/2; (iv) −*x*+1/2, *y*−1/2, −*z*+1/2; (v) −*x*+1/2, −*y*+3/2, −*z*+1.